Separation and Purification Technology 71 (2010) 30–37

Contents lists available at ScienceDirect

Separation and Purification Technology

journal homepage: www.elsevier.com/locate/seppur

Effect of face velocity, nanofiber packing density and thickness on filtration performance of filters with nanofibers coated on a substrate

Wallace Woon-Fong Leung[a,b,*], Chi-Ho Hung[b], Ping-Tang Yuen[a,b]

[a] Room W502a, Research Institute of Innovative Products & Technologies, The Hong Kong Polytechnic University, Hung Hom, Kowloon, Hong Kong
[b] Department of Mechanical Engineering, General Office, 6/F, FG Core, The Hong Kong Polytechnic University, Hung Hom, Kowloon, Hong Kong

ARTICLE INFO

Article history:
Received 6 August 2009
Received in revised form 22 October 2009
Accepted 26 October 2009

Keywords:
Nanofiber
Air filtration
Pressure drop
Electrospinning
Non-woven

ABSTRACT

The objective of this study is to evaluate the effect of face velocity, nanofiber packing density and nanofiber layer thickness on filtration efficiency and pressure drop of filters with nanofibers coated on a substrate. The substrate is a non-woven microfiber medium with negligible filtration efficiency and pressure drop as compared to nanofiber layer. The nanofiber layer is composed of electrospun polyethylene oxide nanofibers with mean diameter equals to 208 nm. Test aerosol is sodium chloride with size ranging from 50 to 480 nm. Experimental results show that the most penetrating particle size decreases from 140 to 90 nm when nanofiber packing density increases from 3.9 to 36×10^{-3}. When face velocity is increased from 5 to 10 cm s^{-1}, the filtration efficiency generally decreases, and the reduction becomes larger at smaller particle sizes especially for those below 100 nm. By maintaining nanofiber packing density at 8.7×10^{-2} and almost triple the nanofiber layer thickness, the most penetrating particle size decreases slightly from 140 to 120 nm. This suggests nanofiber layer thickness has less prominent effect on most penetrating particle size than nanofiber packing density. By adding more nanofibers on microfiber substrate in a single layer especially under high fiber packing, the pressure drop across the filter elevates without significantly improving the filtration efficiency exhibiting a diminishing return behavior. Hence, the method of "multi-layering" is proposed to fabricate nanofiber filter with greatly reduced pressure drop. This is advantageous for high efficiency applications with nanofibers of high packing density.

1. Introduction

Non-woven fibrous filter is a cost-effective means for the collection of particulates from gas stream. Filter quality mainly depends on its filtration efficiency and pressure drop. To improve filter quality, we can either increase the filtration efficiency or reduce the pressure drop, without altering another property. According to filtration theories [1], reduction in fiber size leads to greater filtration efficiency but increased pressure drop when the packing density of fiber is kept constant. The filtration theories validated by test data cover continuum and aerodynamic slip flow regime [2]. For filters operating in transition ($0.25 < Kn < 10$) and molecular ($Kn > 10$) flow regime, there is only limited comparison between theoretical predictions and experimental results during the past. Nanofibers have large surface area-to-volume ratio, and nanofiber media have low basis weight and relatively uniform fiber size, which make them appropriate as a cost effective means in many air filtration applications. However, the homogeneity of fiber packing is the biggest concern. Most researchers postulated that non-woven filters composed of nanofibers, or non-woven microfiber filter integrated with nanofibers, possess greatly enhanced filtration efficiency, but increased pressure drop as a trade-off. Hence, the amount of nanofibers in a filter medium has to be carefully adjusted to prevent incurring excess pressure drop. Past studies have demonstrated the filtration capability of media composed of electrospun Nylon 6 (N6) nanofibers [3] and polyethylene oxide (PEO) nanofibers [4]. In addition, Dharmanolla and Chase [5] reported that it is possible to increase the quality factor (QF) of a microfiber filter by mixing microfibers and electrospun nanofibers through vacuum molding. They have proposed an algorithm to optimize the amount of nanofibers to be added for constructing a filter medium with maximized QF. To further understand the effect of properties such as face (superficial) velocity, fiber packing density and filter thickness on filtration efficiency and pressure drop of nanofiber filters, isolated nanofiber layer has been fabricated in various forms for testing.

Nanofiber medium on itself is soft and fragile and cannot be used alone as air filters. However, nanofibers can be coated on a rigid substrate to form a composite that can be handled readily. Most often the substrate is a non-woven microfiber medium [6–9]. For research purpose, it is desirable to use an extremely permeable

* Corresponding author. Tel.: +852 2766 6670; fax: +852 2365 4703.
E-mail addresses: riwl@polyu.edu.hk (W.W.-F. Leung), 05901927r@polyu.edu.hk (C.-H. Hung), riptyuen@polyu.edu.hk (P.-T. Yuen).

1383-5866/$ – see front matter © 2009 Elsevier B.V. All rights reserved.
doi:10.1016/j.seppur.2009.10.017

microfiber medium with negligible filtration efficiency as the substrate, so that the filtration efficiency and pressure drop measured across the composite can be approximated to those of nanofiber layer [6,7]. Nanofiber coating can be either produced by electrospinning method [10] or melt-blown process [8,9], with diameter of electrospun fibers usually smaller than that of melt-blown fibers.

The objective of this study is to evaluate the effect of face velocity, nanofiber packing density and nanofiber layer thickness on filtration efficiency and pressure drop of filters with nanofibers coated on a substrate. The substrate is a non-woven microfiber medium with negligible filtration efficiency and pressure drop as compared to nanofiber layer. The nanofiber layer was produced by electrospinning using PEO as the polymer. The count mean diameter (CMD) of nanofibers was about 200–300 nm. Samples in various nanofiber packing densities were produced by adopting different electrospinning durations. Efficiency tests were performed using sub-micron sodium chloride (NaCl) aerosol ranging from 50 to 480 nm. Predictions from classical filtration theories were also checked against experimental results, which indicated the need for modification in modeling the capture of sub-micron aerosol by nanofibers.

2. Empirical correlation on filtration efficiency and pressure drop

The filtration efficiency, η, is defined as:

$$\eta = 1 - \frac{C_{down}}{C_{up}} \tag{1}$$

where C_{up} and C_{down} are the number concentration of particles at filter upstream and downstream, respectively.

The quality factor, QF, is defined as:

$$QF = \frac{-\ln(1-\eta)}{\Delta P} \tag{2}$$

where ΔP is the pressure drop across the filter. QF represents the ratio between filtration efficiency measure and pressure drop. A filter with greater filtration efficiency and/or lower pressure drop than another will have higher QF. Thus, a filter of better quality has larger QF.

2.1. Filtration efficiency

The filtration efficiency of a clean non-woven fibrous filter can be approximated by an idealized structure of fibers for which the filtration efficiency (η), fiber packing density (α), single fiber efficiency (η_f), filter thickness (Z) and mean fiber diameter (d_f) are all related as follows [11]:

$$\eta = 1 - \exp\left[-\frac{4\alpha\eta_f Z}{\pi(1-\alpha)d_f}\right] \tag{3}$$

Among various correlation models on η_f, the model as offered by Payet et al. [12] has taken the slip effect into account and shows close agreement with experimental results for particle size range from 80 to 400 nm. For nanofiber filters, the interaction of diffusion and interception is significant, and inertial impaction is usually neglected, i.e.

$$\eta_f = \eta_D + \eta_R \tag{4}$$

where η_D and η_R are the single fiber efficiencies due to diffusion and interception respectively, and are expressed in Eqs. (5) and (6) accordingly:

$$\eta_D = 1.6\left(\frac{1-\alpha}{Ku}\right)^{1/3} Pe^{-2/3} C_1 C_2 \tag{5}$$

where $Ku = -(\ln\alpha)/2 + \alpha - \alpha^2/4 - 3/4$ is the Kuwabara hydrodynamic factor, $Pe = U_0 d_f/D$ is the Peclet number with U_0 as the face velocity, $D = k_B T C_s/3\pi\mu D_p$ is the diffusion coefficient, k_B is the Boltzmann constant, T is the absolute temperature, μ is the air dynamic viscosity, D_p is the particle diameter, $C_s = 1 + Kn[1.207 + 0.44\exp(-0.78/Kn)]$ is the Cunningham slip correction factor according to Rader [13] with $Kn = 2\lambda/D_p$ as the Knudsen number of particle, $C_1 = 1 + 0.388 Kn_f[(1-\alpha)Pe/Ku]^{1/3}$ with $Kn_f = 2\lambda/d_f$ as the Knudsen number of fiber and $C_2 = \frac{1}{1+1.6[(1-\alpha)/Ku]^{1/3} Pe^{-2/3} C_1}$.

$$\eta_R = 0.6\left(\frac{1-\alpha}{Ku}\right)\left(1 + \frac{Kn_f}{D_p/d_f}\right)\left(\frac{D_p^2/d_f^2}{1 + D_p/d_f}\right) \tag{6}$$

where D_p/d_f is sometimes referred as the interception ratio.

2.2. Pressure drop

Davies' [14] empirical formula of pressure drop ΔP across a clean fibrous filter is:

$$(\Delta P) d_f^2/(4\mu U_0 Z) = 16\alpha^{1.5}(1 + 56\alpha^3) \tag{7}$$

Eq. (7) is obtained by Davies [14] through testing of fibrous filter with d_f ranging from 1.6 to 80 μm and α smaller than 0.3. Pressure drop across a clean fibrous filter measured experimentally should be within ±30% [14] to that estimated from Eq. (7), provided that 1.6 μm < d_f < 80 μm and 0.006 < α < 0.3. Subsequently, Davies' correlation was further validated by Werner and Clarenburg [15] to cover the finer range on fiber diameter (98 nm < d_f < 1.54 μm and 0.039 < α_f < 0.084). Since

$$\alpha = \frac{W}{\rho_f Z} \tag{8}$$

where W is the mass of fibers per unit filter area (basis weight) and ρ_f is the fiber material density, Eq. (7) can be re-written as:

$$\frac{(\Delta P) d_f^2 \rho_f}{4\mu U_0 W} = 16\alpha^{0.5}(1 + 56\alpha^3) \tag{9}$$

By knowing W and ρ_f beforehand and after measuring ΔP across the filter, α can be estimated according to Eq. (9). This is an estimation using Davies' equation.

3. Experimental

3.1. Fabrication of polyethylene oxide nanofiber filter

Fig. 1 shows a schematic of the nanofiber electrospinning unit (NEU-010, KES Kato Tech Co., Ltd.). The 20 ml syringe is filled with polyethylene oxide (PEO) solution. Its plunger is adhered to a linear actuator system in which the solution feed rate can be carefully adjusted and maintained steady throughout the electrospinning process. The capillary is connected to a high voltage supply and the drum is ground as a collector. An electric potential is generated between the capillary and the drum. Solution that flows out slowly from the capillary is subjected to an electric force. The hemispherical solution droplet attached to the outlet of capillary then deforms into conical shape, which is known as the Taylor cone. A jet is produced when the electric force overcomes the surface tension of the Taylor cone. The jet travels through the air towards the rotating drum, where the substrate is wrapped around. Adjacent like charges deposited on the fiber repels against each other stretching the fiber and producing even smaller-diameter sub-branches. This whole process continues until the jets or smaller jets hit the collector surface. At the same time, solvent evaporation in flight

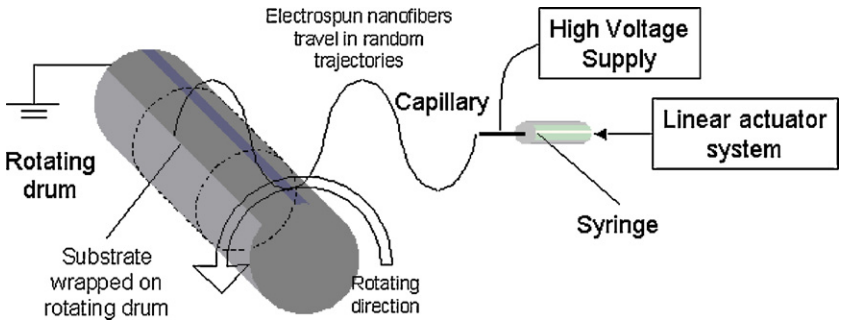

Fig. 1. Schematic of the nanofiber electrospinning unit.

is enhanced as the sub-jets have large surface area leading to only polymer nanofibers deposited on the substrate surface. The syringe is set into transverse motion along the rotating axis of the drum to achieve wider covering of nanofibers on the substrate.

The conditions to electrospin PEO nanofibers are determined by referencing to Wan et al. [16], Doshi and Reneker [17] and Tsai et al. [4], accompanied by our repeated trials and inspection of samples under Scanning Electron Microscope (SEM) to observe for uniform fiber diameter with minimum bead formation. PEO solution is prepared by dissolving PEO powders (obtained from Aldrich) having a molecular weight of 600,000 g/mol in a solvent containing 80 vol.% of isopropyl alcohol and 20 vol.% of water. The mass ratio between polymer and solvent is 5%. The syringe has 20 ml nominal volume and the capillary is of 0.7 mm inner diameter. The applied voltage is 20 kV and the distance between capillary and drum surface is 14 cm. Solution feed rate is maintained at 6×10^{-3} ml/min. The substrate is a non-woven composed of coarse fibers with mean diameter at 14.7 μm. Pressure drop across the substrate at 5 cm s^{-1} is measured to be 1.39 Pa.

Nanofiber packing density depends on electrospinning duration. The longer the electrospinning lasts, the more nanofibers can be coated on the substrate. The basis weight W of nanofibers as described in Eqs. (9) and (10) thus increases with electrospinning duration. It is intuitive to assume both the packing density α and thickness Z of the nanofiber layer increase with electrospinning duration. To fabricate nanofiber layers of the same α but different Z, nanofiber filters (i.e. substrate coated with nanofibers) produced under the same electrospinning duration can be stacked up as depicted in Fig. 2. Practically, the nanofiber layer in the stack can be considered to have packing density and thickness close to α and $2Z$.

3.2. Performance evaluation of nanofiber filter

Sub-micron aerosol generator (SMAG 7388L, MSP Corp.) containing an atomizer and electrostatic classifier is used to generate sodium chloride (NaCl) test aerosol ranging from 50 to 480 nm diameter. Condensation particle counter (CPC 3010, TSI Inc.) is used to measure particle number concentration. Pressure drop across test filter is measured by capillary flow porometer (CFP-1100A, PMI). Substrate thickness is measured by micrometer. Face velocity in the test is adjusted through the throttle valve on the rotameter. The filters are tested under face velocities of 5 and 10 cm s^{-1}, respectively. Make-up air stream is filtered by HEPA filter to ensure that no particle species other than NaCl are present in the aerosol stream. Isokinetic sampling tube is used for getting representative readings of particle concentrations. Mean fiber diameter is estimated from pictures obtained by SEM (JSM 6490, JEOL).

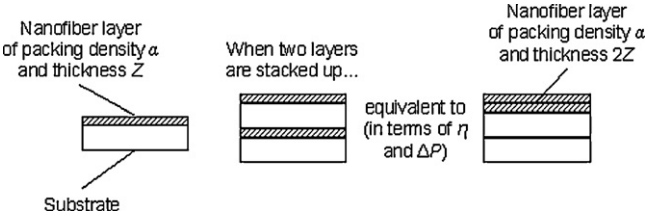

Fig. 2. Nanofiber layer of the same packing density but different thickness.

The test filter is clamped within an air-tight test rig and tested for filtration efficiency with NaCl particles ranging from 50 to 480 nm diameter. The experimental set-up is shown in Fig. 3. The aerosol output from electrostatic classifier passes through another aerosol neutralizer (Po-210) to reach the Boltzmann equilibrium charged state before mixing up with make-up air stream. The charge effect of test aerosol should be negligible. Moreover, PEO nanofibers produced from electrospinning has poor charge retention property [4]. Hence, the filtration mechanism in our study can be regarded as purely mechanical in nature. CPC is used to measure particle number concentration at filter upstream and downstream alternatively. Multiple charge effect needs to be corrected in order to obtain the actual particle number concentration. Details are given in Appendix A.

4. Results and discussion

4.1. Physical parameters of nanofiber filters

Table 1 summarizes the physical parameters of substrate and nanofiber layers coated on it. The substrate is obtained from manufacturer and the nanofiber layers (N1–N9) are produced in our laboratory by electrospinning PEO solution under the conditions mentioned in Section 3.1. N1 to N9 are produced under different electrospinning durations, with N1 the shortest and gradually increases to N9. The basis weight W of substrate is measured by electronic balance, while the values of nanofiber layers are too small to be detectable. Instead, W of N1 to N9 was determined by multiplying the solution feed rate (6×10^{-3} ml/min), solvent density, polymer/solvent mass ratio (5%) and electrospinning duration together. Thus, W is proportional to electrospinning duration. The mean fiber diameter d_f is estimated from SEM pictures. Since the nanofiber layers are coated on substrates, pressure drop ΔP across the nanofiber layers cannot be measured directly. Instead, the ΔP across clear substrate was first measured, and this value was being subtracted from the ΔP across substrates coated with nanofibers (i.e. composites). For example, ΔP across substrate coated with nanofiber layer N3 is measured to be 14.6 Pa at 5 cm s^{-1}, and the ΔP across a clear substrate of 1.4 Pa is being subtracted to yield the ΔP across N3 being 13.2 Pa. The thickness Z of the substrate on the order of mm is measured by micrometer. Its packing density α is estimated from Eq. (7) by knowing $\Delta P/U_0$, d_f and Z. It is very difficult to use the SEM (cross-section) to measure the thickness of

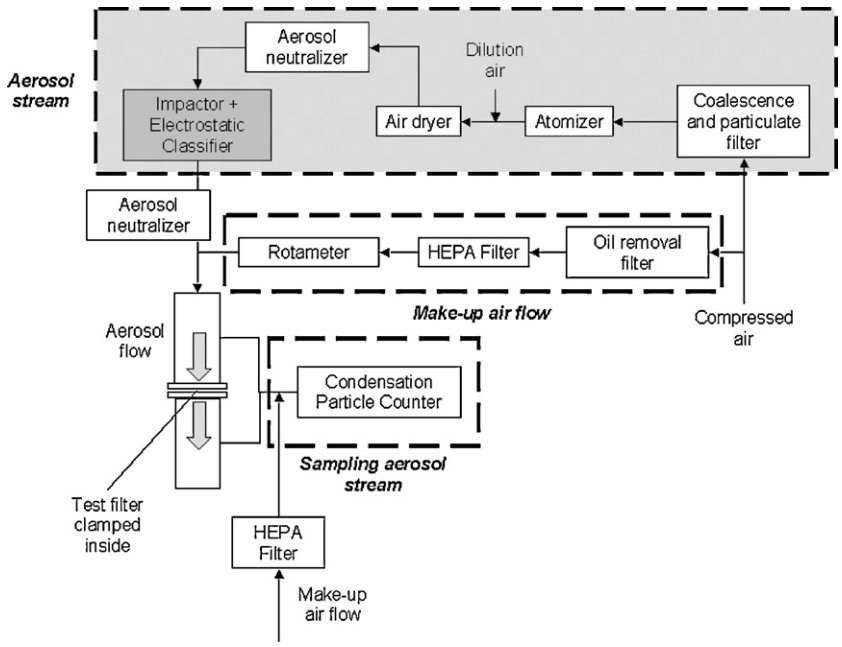

Fig. 3. Experimental set-up for testing of filtration efficiency.

nanofiber layer because the nanofibers coated on substrate are very thin and easily damaged during the cutting process, thus the cross-section of nanofiber layer as viewed under SEM is heavily deformed. For example, N3 has d_f equals to 208 nm, W equals to 0.12 g m^{-2}, ρ_f equals to 1.22 g cm^{-3} and ΔP equals to 13.2 Pa when $U_0 = 5$ cm s^{-1}. Hence, its α is estimated to be 8.7×10^{-3} from Eq. (9). It follows that Z as obtained from Eq. (8) equals to 11.8×10^{-6} m. Values of α and Z obtained in this way should be allowed for variances. Nevertheless, we must estimate α and Z of nanofiber layers, as they are essential in modeling the filtration efficiencies. The uncertainty of ΔP is obtained from repeated measurements on the same sample. The uncertainties of derived quantities α and Z are obtained from experimental uncertainty analysis. Fig. 4a–c are the SEM pictures (top view of nanofiber layer) of N1S, N4S and N8S, respectively. While the substrate fibers can still be observed in pictures of N1S and N4S, they are completely covered up by nanofibers in N8S, indicating the increasing basis weight of nanofibers.

By considering only the nanofiber layer, Fig. 5 shows that α increases with W but the increase rate drops subsequently after $W = 0.4$ g m^{-2}. On the other hand, Fig. 6 shows that Z starts to increase after $W = 0.4$ g m^{-2}.

4.2. Filtration performance vs. nanofiber packing density

Fig. 7 shows the experimental filtration efficiencies at face velocity of 5 cm s^{-1} of clear substrate and substrates coated with nanofibers, together with predictions (continuous curves) from the empirical correlation [Eqs. (3)–(6)] described in Section 2.1. Noted "N1S" represents the composite formed by coating nanofiber layer N1 on substrate S. Experimental results indicate that clear substrate offers negligible filtration efficiency (less than 2%) compared to composites. It follows that the filtration efficiency as measured across composites can be approximated to that of nanofiber layers. As expected, the efficiency curve shifts upward from N1S to N9S due to an increase in basis weight of nanofibers. Nanofiber coating enhances the filtration efficiency of microfiber substrate, also reduces the most penetrating particle size (MPPS) down to 140 nm. Other studies [6–8] also showed that composites formed by coating nanofibers on microfiber substrate always have MPPS lower than conventional microfiber filters.

Since N1S to N9S are dual-layer composites, their theoretical efficiencies are given by:

$$\eta_C = 1 - (1 - \eta_N)(1 - \eta_S) \tag{10}$$

where η_C is the filtration efficiency of composite, η_N and η_S are the filtration efficiencies of nanofiber layer and substrate, respectively, each determined according to the empirical correlation [Eqs. (3)–(6)] described in Section 2. Kn_f of substrate is 9×10^{-3} ($d_f = 14.7$ μm), thus the flow over fibers belongs to aerodynamic slip flow regime ($0.001 < Kn_f < 0.25$). Hence, the model built upon Navier–Stokes equation with slip correction is suitable to predict the filtration efficiency of substrate. On the other hand, Kn_f of nanofiber layer is 0.64 ($d_f = 208$ nm), making the flow over fibers transitional (i.e. transition from slip to molecular flow) which is

Table 1
Physical parameters of substrate and nanofiber layers coated on it.

Medium	Substrate	N1	N2	N3	N4	N5	N6	N7	N8	N9
Mean fiber diameter, d_f (nm)	14.7×10^3	208	208	208	208	208	208	208	208	208
Basis weight, W (g m^{-2})	29.08	0.058	0.088	0.12	0.18	0.23	0.35	0.47	0.58	0.70
Fiber packing density, $\alpha \pm \Delta\alpha$ ($\times 10^{-3}$)	130 ± 4.1	3.9 ± 0.21	6.6 ± 0.29	8.7 ± 0.45	13.6 ± 0.27	17.8 ± 0.44	25.4 ± 0.28	30.8 ± 0.26	34.6 ± 0.31	36.0 ± 0.24
Thickness, $Z \pm \Delta Z$ ($\times 10^{-6}$ m)	100 ± 4	13.3 ± 0.72	11.8 ± 0.52	11.8 ± 0.60	11.4 ± 0.23	11.6 ± 0.29	12.2 ± 0.14	13.4 ± 0.11	14.9 ± 0.13	17.2 ± 0.11
Pressure drop ΔP at 5 cm s^{-1} (Pa)	1.4 ± 0.08	4.4 ± 0.12	8.6 ± 0.19	13.2 ± 0.34	24.7 ± 0.25	37.7 ± 0.47	67.6 ± 0.38	99.4 ± 0.42	131.8 ± 0.61	161.2 ± 0.55

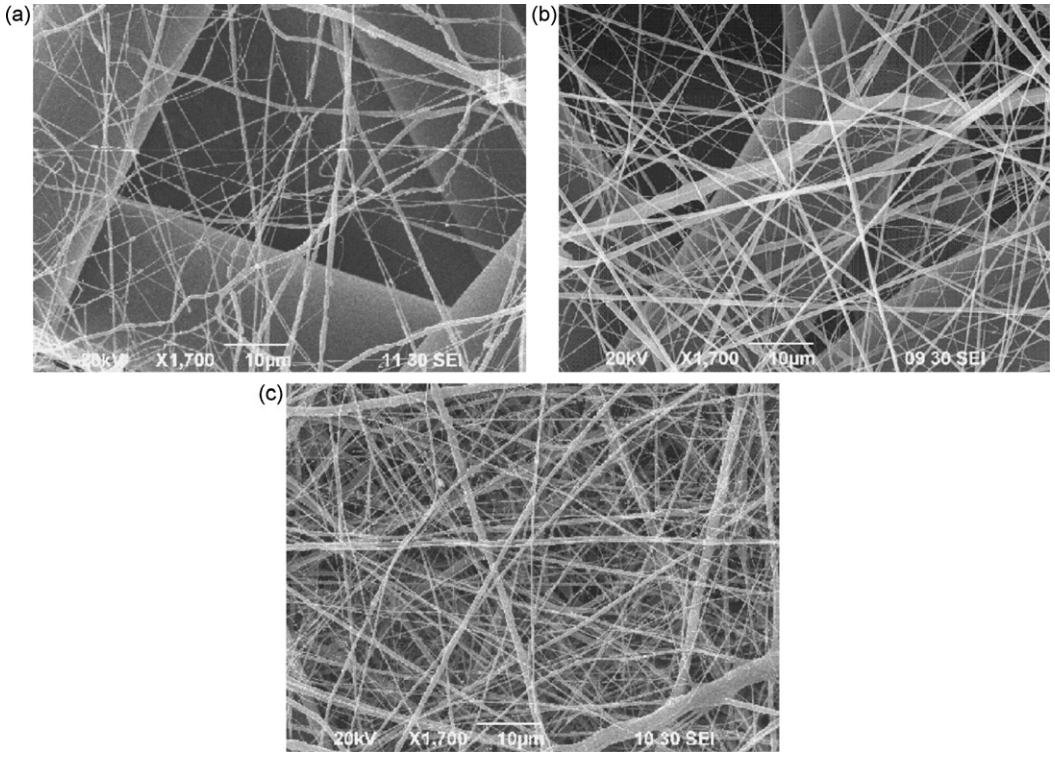

Fig. 4. SEM pictures of (a) N1S, (b) N4S, and (c) N8S.

difficult to simulate, and the model is not a physical representation on flow problem in nano-scale. Moreover, our test aerosol is submicron in size from 50 to 480 nm. It follows that aerosols and fibers are of similar scale and aerosols can no longer be treated as point masses not affecting the flow over fibers, which contradicts with model's assumption. Despite this, the theoretical and experimental filtration efficiency of composite containing nanofiber layer are still compared to determine the possible deviation. Surprisingly, the model can predict quite accurately the filtration efficiencies for D_p smaller than 100 nm over the whole test range on nanofiber packing density. For D_p larger than 300 nm, the experimental efficiency curve agrees with theoretical one over the range of nanofiber packing density from 3.9 (N1S) to 8.7×10^{-3} (N3S). Starting from 13.6×10^{-3} (N4S), the model over-estimates filtration efficiencies for D_p larger than 300 nm and the deviation grows with particle size. This over-estimation even starts early at $D_p = 200$ nm when nanofiber packing density equals to 36.0×10^{-3} (N9S). Hence, the model seems to over-estimate the interception effect offered by nanofiber in capturing particles larger than its diameter especially under higher nanofiber packing condition.

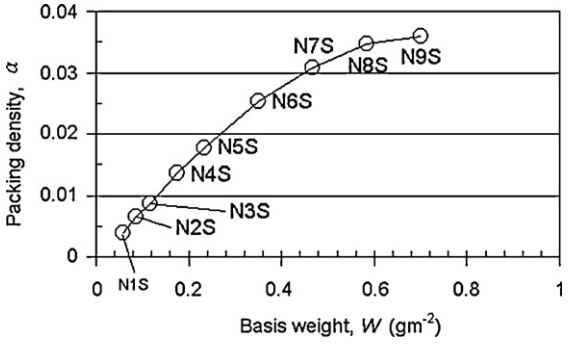

Fig. 5. Packing density α against basis weight W of nanofiber layer.

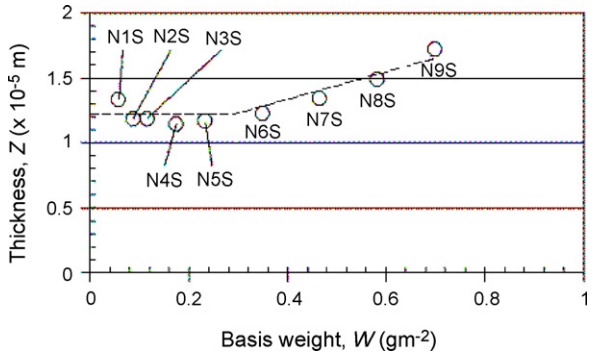

Fig. 6. Thickness Z against basis weight W of nanofiber layer.

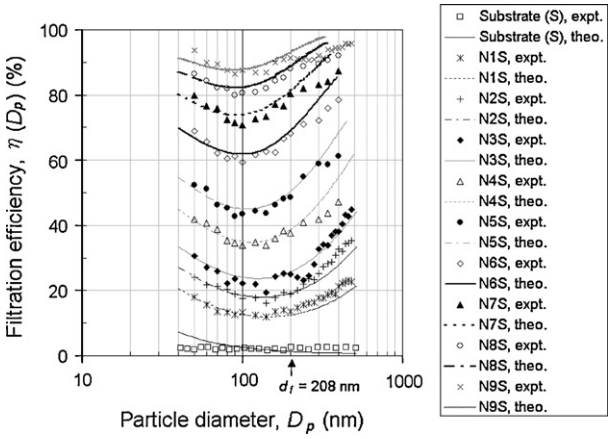

Fig. 7. Filtration efficiencies of clear substrate (S) and substrates coated with nanofibers (N1S to N9S).

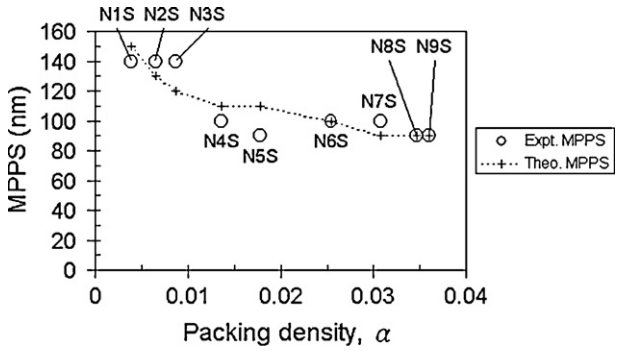

Fig. 8. MPPS as a function of nanofiber packing density.

The theoretical MPPS can be obtained by differentiating Eq. (3) with respect to D_p and set to zero, or just by inspection from the theoretical efficiency curve. In Fig. 8, the dotted line connecting theoretical MPPS of N1S to N9S shows a generally decreasing trend against nanofiber packing density, where experimental results also agree with the trend.

4.3. Filtration performance vs. face velocity

Fig. 9a compares the filtration efficiencies under face velocities of 5 and 10 cm s^{-1}. Experimental results show that filtration efficiencies over particle size range from 50 to 480 nm generally decrease with respect to increase in face velocity from 5 to 10 cm s^{-1}. This phenomenon occurs for all composites, despite only

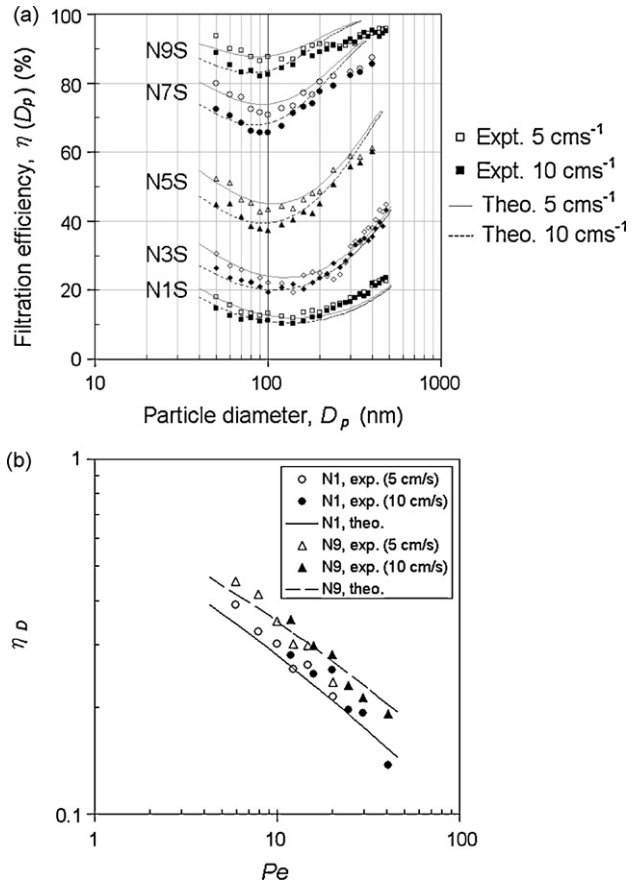

Fig. 9. (a) Filtration efficiencies of N1S, N3S, N5S, N7S and N9S under face velocities of 5 and 10 cm s^{-1}. (b) Comparison of experimental and theoretical η_D of nanofiber layers N1 and N9.

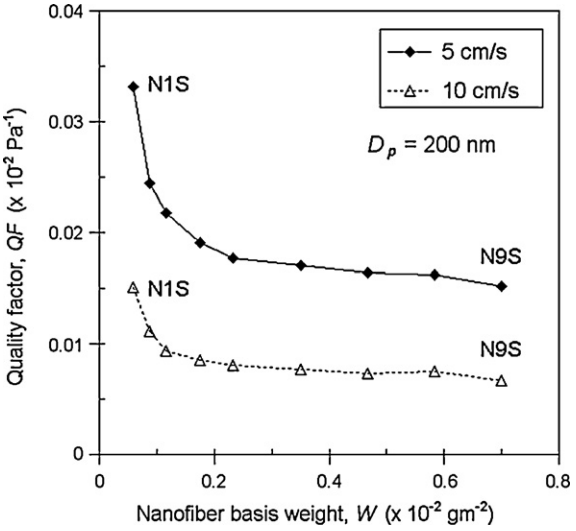

Fig. 10. Quality factor against nanofiber basis weight under face velocities of 5 and 10 cm s^{-1}.

the results of N1S, N3S, N5S, N7S and N9S are depicted in Fig. 8. The reduction on filtration efficiency becomes larger at smaller particle sizes. This is in agreement with theoretical prediction because doubling the face velocity is equivalent to reducing by a factor of half the retention time of particles in the nanofiber filter, thus lowers the chance for particles to collide on fibers through Brownian motion (diffusion). Since diffusion is the dominating capture mechanism for particles smaller than 100 nm, the filtration efficiencies of these particles are mostly affected. For particles larger than 300 nm, the filtration efficiencies remain nearly unchanged when face velocity increased from 5 to 10 cm s^{-1}. This is due to the fact that the Reynolds number (Re) based on the nanofiber diameter ranges between 7×10^{-4} and 1.4×10^{-3} which is under creeping low Reynolds number flow ($Re \ll 1$) and the streamlines in such flow field does not change, hence capture, by the nanofiber, of the aerosol as carried by the stream flow (i.e. interception) remains unchanged.

When face velocity increased from 5 to 10 cm s^{-1}, the model still generates efficiency curve that closely agrees with experimental values for composites N1S and N3S. However, predicted efficiency curve starts to deviate from experimental values at larger particle sizes as nanofiber packing density increases. This has been observed in the case of 5 cm s^{-1} in Section 4.2. The same observation under 10 cm s^{-1} further implies that assumed flow independence between larger particles and smaller fibers cannot be hold when nanofibers become more closely packed. Fig. 9b plots experimental and theoretical η_D against Peclet number (Pe) of nanofiber layers N1 and N9. Theoretical η_D is predicted by Eq. (5). Experimental η_D is obtained by first back-calculate single fiber efficiency η_f from experimental filtration efficiency η using Eq. (3), followed by subtracting η_R [Eq. (4)] from η_f. It shows the applicability of Eq. (5) to nanofiber filters when Pe is smaller than 50.

Fig. 10 shows the quality factor (QF) at a particle size of 200 nm as a function of nanofiber basis weight (W) under face velocities of 5 and 10 cm s^{-1}. From Darcy's Law, pressure drop across filter increases linearly with face velocity. As shown in Fig. 9a, filtration efficiency generally decreases with respect to increase in face velocity. Hence, quality factor as an indicator to filtration performance should become lower at higher face velocity, which is depicted in Fig. 10. QF of nanofiber filter decreases with W, and most rapidly at initial values of W. This trend follows when face velocity increases to 10 cm s^{-1}, but subjected to a lower decrease rate. To have better filtration performance, it is recommended to adopt the lowest

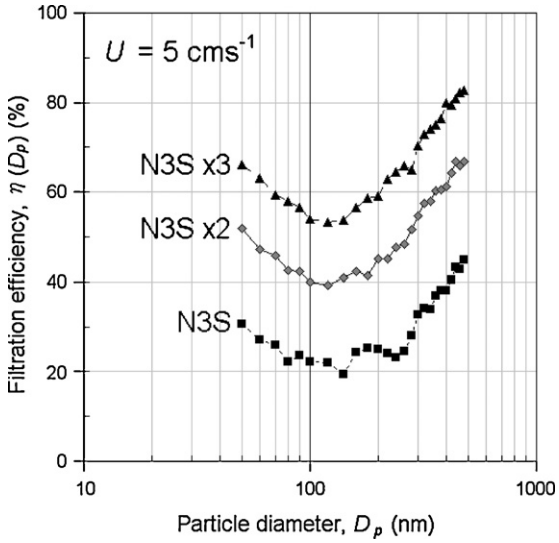

Fig. 11. Filtration efficiencies of N3S, N3S ×2 and N3S ×3 under face velocity of 5 cm s^{-1}.

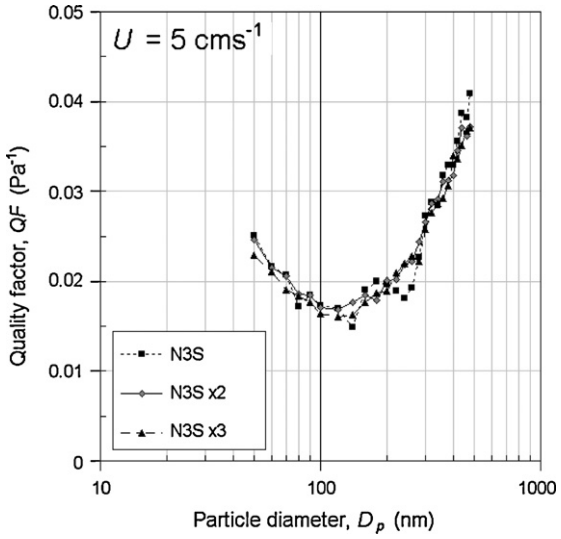

Fig. 12. Quality factors of N3S, N3S ×2 and N3S ×3 under face velocity of 5 cm s^{-1}.

possible face velocity when nanofiber filter is used. In addition, it is more cost-effective to use lower basis weight of nanofibers due to the relatively higher *QF*, which is the basis of multi-layer filter using multiple low-basis weight nanofiber layers to be discussed later.

4.4. Filtration performance vs. thickness of nanofiber layer

Two and three layers of N3S (so-called N3S ×2 and N3S ×3) are stacked up in order to form nanofiber layers with the same packing density but increased thickness as compared to single layer of N3S. Given the filtration efficiency and pressure drop across a filter as η and ΔP, respectively, it can be deduced from Eq. (2) that the quality factor of a composite formed by stacking up k identical layers of the filter remains unchanged, i.e.

$$QF_k = -\frac{\ln(1-\eta)^k}{k(\Delta P)} = -\frac{\ln(1-\eta)}{\Delta P} = QF \tag{11}$$

Fig. 11 shows the filtration efficiencies of N3S, N3S ×2 and N3S ×3 at 5 cm s^{-1}. Practically, nanofiber packing density (α) remains close to 8.7×10^{-3}, while nanofiber layer thickness (Z) and basis weight (W) increase in discrete multiples. Pressure drop measured across N3S ×2 and N3S ×3 are 29.75 and 47.23 Pa, respectively, which are close to two and three times of ΔP across N3S (14.58 Pa). ΔP across individual N3S layers in N3S ×2 and N3S ×3 have also been measured. In N3S ×2, they are 15.44 and 14.31 Pa, thus making up to 29.75 Pa. In N3S ×3, they are 16.53, 14.7 and 16 Pa, thus making up to 47.23 Pa. Hence, ΔP measured across the individual N3S layers are 14.58, 15.44, 14.31, 16.53, 14.7 and 16 Pa, respectively. The average is 15.26 Pa with a standard deviation equal to 0.80 Pa. It shows the variation in ΔP of each layer, which indicates the inevitable inhomogeneity of nanofiber packing as resulted from the random nature of electrospinning process. The MPPS of N3S is 140 nm and decreased slightly to 120 nm when Z is doubled. When Z is tripled, MPPS remains at 120 nm. It is believed that the effect of Z on MPPS is less prominent than that of α (as depicted in Fig. 7). Fig. 12 shows the experimental quality factors of N3S, N3S ×2 and N3S ×3, which are close to each other as expected from Eq. (11).

The circles in Fig. 13 represent the experimental filtration efficiencies (of 200-nm aerosol) and pressure drop of N1S to N9S single layer nanofiber filter. These data points are linked up to show the diminishing return characteristic of nanofiber filter. By adding more nanofibers, the filtration efficiency increases in a decreasing rate with respect to pressure drop. It means that nanofibers deposited as single layer elevate the pressure drop without significantly improving the filtration efficiency, which lowers the quality factor and leads to poorer performance, especially when nanofiber basis weight is high (see Fig. 10). This problem may hinder the use of nanofibers in high performance filtration. However, Eq. (11) shows that stacking up multiple filters does not alter the quality factor, and this postulation has been verified by experiment results as depicted in Fig. 12. Hence, it is prudent to investigate the pressure drop savings that can be achieved through "multi-layering". In Fig. 13, the dotted curve represents the projection when multiple units of N1S (W = 0.058 g m^{-2}) with high QF are stacked up. Under the same W of 0.70 g m^{-2}, N1S ×12 provides a pressure drop savings by 93.12 Pa, with filtration efficiency at 82.60%, which is slightly lower than that of N9S at 91.37%. When W is equal to 0.23 g m^{-2}, pressure drop savings offered by N1S ×4 as compared to N5S is 15.90 Pa, with filtration efficiency drops from 48.69 to 44.17%. It can be observed that ΔP savings through "multi-layering" become more significant at higher W. In addition, irrespective of single- or multi-layer nanofiber filter, they perform better than microfiber filter, as depicted in Fig. 12. As mentioned before, nanofibers are soft and their non-wovens produced from electrospinning have fixed packing density and thickness at each basis weight. Hence, "multi-layering" can also be regarded as an alternative to adjust the packing density and thickness of nanofiber layer under a fixed basis weight while yielding high efficiency and low pressure drop [18].

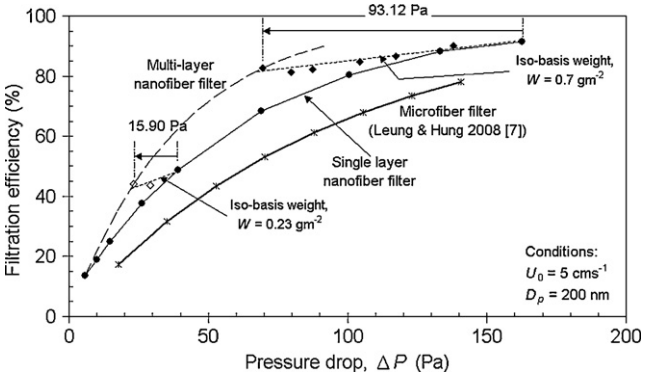

Fig. 13. Operation curves (U_0 = 5 cm s^{-1}, D_p = 200 nm) of multi-layer filters formed by stacking up constituent units from N1S to N9S.

5. Conclusions

The objective of this study has been covered. Nanofiber filters are fabricated by electrospinning PEO nanofibers on microfiber substrate. The mean diameter of PEO nanofibers is 208 nm, by which fluid flow around fibers falls under the transition regime. Firstly, the effect of nanofiber packing density on filtration performance has been investigated. Both experiment and theory shows that the MPPS decreases with nanofiber packing density. Secondly, the effect of face velocity on filtration performance has been studied. Filtration efficiency generally decreases with face velocity, and the reduction becomes larger at smaller particle sizes. This agrees with theoretical prediction. It is because increased face velocity reduces the retention time of particles within the nanofiber structure, thus lowers the chance for particles to collide on fibers through Brownian motion. In addition, it is recommended to adopt the lowest possible face velocity when nanofiber filter is used; otherwise the quality factor drops dramatically. Thirdly, the effect of nanofiber layer thickness on filtration performance has been investigated. Results show that the effect of nanofiber layer thickness on MPPS is less prominent than that of nanofiber packing density. By adding more nanofibers on microfiber substrate, the filtration efficiency increases in a decreasing rate with respect to pressure drop. It means that nanofibers being deposited into single layer elevate the pressure drop without significantly improving the filtration efficiency, which lowers the quality factor and leads to poorer performance. The performance can be improved by distributing the same amount of nanofibers sparsely through stacking up multiple filters, known as "multi-layering". Pressure drop savings through "multi-layering" becomes more significant at higher nanofiber basis weight or applications that require high efficiency. In addition, under the same amount of nanofibers, stack up constituent units with lower nanofiber basis weight will enhance the pressure drop savings. Alternatively, a multi-layer nanofiber filter can be realized wherein the pressure drop is the same as a single-layer nanofiber filter yet the capture efficiency for submicron aerosol is significantly higher by packing additional nanofiber in the filter.

Appendix A.

To measure the fractional efficiency of a filter, monodisperse NaCl aerosol of specific size is generated from electrostatic classification. Due to multiple charge effect, the resultant aerosol stream always contains particles of the same electrical mobility but different sizes and charges. For example, the stream corresponds to 50 nm aerosol actually composed of 50 nm (+1 charged), 73 nm (+2), 92 nm (+3), 108 nm (+4), 124 nm (+5) and 138 nm (+6) particles. Multiple charge effect at filter upstream can be corrected by using Wiedensohler [19] approximation. However, the filter under test will screen out particles to different extent depending on particle sizes; another method is thus required to determine the actual concentration at filter downstream from particle counter reading.

Suppose the filter upstream and downstream number concentration of 460 nm (+1) and 480 nm (+1) particles have been measured, the corresponding fractional efficiencies $\eta(460)$ and $\eta(480)$ can be determined directly from Eq. (1) due to the fact that their multiply charged (+2, +3, +4, . . .) particles are larger than impactor's cut-off size.

However, the 280 nm aerosol stream actually contains 280 nm (+1), 467 nm (+2) and 648 nm (+3) particles. By neglecting 648 nm (+3) particles due to its relatively low concentration in the aerosol stream, the relationship between particle counter reading and actual concentration is given by:

$$C_{u,reading} = C_u(280_{+1}) + C_u(467_{+2}) \quad (A.1)$$

$$C_{d,reading} = C_d(280_{+1}) + C_d(467_{+2}) \quad (A.2)$$

where $C_{u,reading}$ and $C_{d,reading}$ are the upstream and downstream number concentrations as shown on the particle counter, respectively. $C_u(467_{+2})$ is the upstream concentration of +2 charged 467 nm particles which is in a fixed proportion to $C_u(467_{+1})$ under the standard bi-polar charge distribution. $C_u(467_{+1})$ is obtained by interpolation using $C_u(460_{+1})$ and $C_u(480_{+1})$. $C_u(280_{+1})$ is then obtained from Eq. (A.1). $C_d(467_{+2})$ is equal to $C_u(467_{+2})$ times $1-\eta(467)$, as interpolated from $\eta(460)$ and $\eta(480)$. $C_d(280_{+1})$ is then determined according to eq. (A.2). Both $C_u(280_{+1})$ and $C_d(280_{+1})$ are substituted into Eq. (1) giving $\eta(280)$. The above steps are repeated to obtain fractional efficiencies from large to small particle sizes until the whole test range has been covered.

References

[1] W.C. Hinds, Aerosol Technology, second ed., Wiley-Interscience, New York, 1998.
[2] A.A. Kirsch, I.B. Stechkina, in: D.T. Shaw (Ed.), Fundamentals of Aerosol Science, John Wiley & Sons, New York, 1978, pp. 165–256.
[3] J.K. Lee, Y.C. Ahn, S.K. Park, G.T. Kim, Y.H. Hwang, C.G. Lee, H.S. Shin, Development of high efficiency nanofilters made of nanofibers, Curr. Appl. Phys. 6 (2006) 1030–1035.
[4] Peter P. Tsai, H. Schreuder-Gibson, P. Gibson, Different electrostatic methods for making electret filters, J. Electrostat. 54 (2002) 333–341.
[5] S. Dharmanolla, G.G. Chase, Computer program for filter media design optimization, J. Chin. Inst. Chem. Eng. 39 (2008) 161–167.
[6] J. Wang, C.K. Seong, D.Y.H. Pui, Investigation of the figure of merit for filters with a single nanofiber layer on a substrate, J. Aerosol Sci. 39 (2008) 323–334.
[7] W.F. Wallace, C.H. Leung, Hung, Investigation on pressure drop evolution of fibrous filter operating in aerodynamic slip regime under continuous loading of sub-micron aerosols, Sep. Purif. Technol. 63 (2008) 691–700.
[8] A. Podgórski, A. Bałazy, L. Gradoń, Application of nanofibers to improve the filtration efficiency of the most penetrating aerosol particles in fibrous filters, Chem. Eng. Sci. 61 (2006) 6804–6815.
[9] L. Gradoń, A. Podgórski, A. Bałazy, Filtration of nanoparticles in the nanofibrous filters, in: FILTECH EUROPA 2005, volume II, 2005, pp. 178–185.
[10] T. Subbiah, G.S. Bhat, R.W. Tock, S. Parameswaran, S.S. Ramkumar, Electrospinning of nanofibers, J. Appl. Polym. Sci. 96 (2005) 557–569.
[11] R.C. Brown, Air Filtration: An Integrated Approach to the Theory and Applications of Fibrous Filters, Pergamon Press, Oxford, 1993.
[12] S. Payet, D. Bouland, G. Madelaine, A. Renoux, Penetration and pressure drop of a HEPA filter during loading with submicron liquid particles, J. Aerosol Sci. 23 (1992) 723–735.
[13] D.J. Rader, Momentum slip correction factor for small particles in nine common gases, J. Aerosol Sci. 21 (1990) 161–168.
[14] C.N. Davies, The separation of airborne dust and particulates, Proc. Inst. Mech. Eng. Part 1B (1952) 185–213.
[15] R.M. Werner, L.A. Clarenburg, Aerosol filters. Pressure drop across single-component glass fiber filters, Ind. Eng. Chem. Proc. Des. Dev. 4 (1965) 288–293.
[16] Y.Q. Wan, J.H. He, J.Y. Yu, Y. Wu, Electrospinning of high-molecule PEO solution, J. Appl. Polym. Sci. 103 (2007) 3840–3843.
[17] J. Doshi, D.H. Reneker, Electrospinning process and applications of electrospun fibers, J. Electrostat. 35 (1995) 151–160.
[18] Wallace W.F. Leung, C.H. Hung, Multilayer nanofiber filter, US Patent Application Filed May 7, 2009.
[19] A. Wiedensohler, An approximation of the bipolar charge distribution for particles in the submicron size range, J. Aerosol Sci. 19 (1988) 387–389.